Simulations of background sources in AMoRE-I experiment

A. Luqman[a], D.H. Ha[a], J.J. Lee[b], E.J. Jeon[c,*], H.S. Jo[c], H.J. Kim[a], Y.D. Kim[c,d], Y.H. Kim[c,e], V.V. Kobychev[f], H.S. Lee[c], H.K. Park[c], K. Siyeon[b], J.H. So[c], V.I. Tretyak[f], Y.S. Yoon[c,*]

[a]*Department of Physics, Kyungpook National University, DaeGu 41566, Korea*
[b]*Department of Physics, Chung-Ang University, Seoul 06974, Korea*
[c]*Center for Underground Physics, Institute for Basic Science, Daejeon 34047, Korea*
[d]*Department of Physics, Sejong University, Seoul 05006, Korea*
[e]*Korea Research Institute of Standards and Science, Daejeon 34113, Korea*
[f]*Institute for Nuclear Research, MSP 03680 Kyiv, Ukraine*

Abstract

The first phase of the Advanced Mo-based Rare Process Experiment (AMoRE-I), an experimental search for neutrinoless double beta decay ($0\nu\beta\beta$) of ^{100}Mo in calcium molybdate (CMO) crystal using cryogenic techniques, is planned at the YangYang underground laboratory (Y2L) in South Korea. A GEANT4 based Monte Carlo simulation was performed for the first-phase the AMoRE-I detector and shield configuration. Background sources such as ^{238}U, ^{232}Th, ^{40}K, ^{235}U, and ^{210}Pb were simulated from inside the crystals, surrounding materials, outer shielding walls of the Y2L cavity; background rates in the region of interest were estimated. The estimated background rate in the region of interest was estimated to be $<1.18 \times 10^{-3}$ counts/keV/kg/yr (ckky). The effects of random coincidences between background and two-neutrino double beta decay of ^{100}Mo were estimated as a potential background source and its estimated rate was $<2.26 \times 10^{-4}$ ckky.

Keywords: Backgrounds, Simulation, Double beta decay, Underground experiment, CaMoO$_4$ crystals

*Corresponding author
Email addresses:* `ejjoon@ibs.re.kr` (E.J. Jeon), `ysy@ibs.re.kr` (Y.S. Yoon)

1. Introduction

As of today, on the basis of results from a number of neutrino oscillation experiments, it is known that neutrinos have mass. However, their absolute mass scale is still not known [1, 2]. The half-life of neutrinoless double beta decay $(0\nu\beta\beta)$ of certain nuclei is related to the effective Majorana neutrino mass, and the investigation of neutrinoless double beta decays is the only practical way to determine the absolute neutrino mass scale and the nature of the neutrino such as Majorana or Dirac particle [2]. The Advanced Mo-based Rare Process Experiment (AMoRE) [3] is an experimental search for neutrinoless double beta decay of ^{100}Mo nuclei using $CaMoO_4$ (CMO) scintillating crystals operating at milli-Kelvin temperatures and is planned to operate at the YangYang underground laboratory (Y2L) in South Korea. The AMoRE experiment will be done in a series of phases; the first phase of the experiment (AMoRE-I) will use a ~5 kg (possibly, up to 10 kg) array of CMO crystals. The goal of a background level for AMoRE-I is 0.002 counts/keV/kg/yr (ckky) in the region of interest (ROI), 3.034 ± 0.01 MeV. Radiation originating within the $CaMoO_4$ crystals will probably be the dominant source of backgrounds. These include emanations from radioisotopes contained in the ^{238}U, ^{232}Th, and ^{235}U decay chains as well as ^{40}K from materials in the nearby detector system and the internal lead shielding plate, the G10 fiberglass components of the cryogenic system, and the outer lead shielding box that produce signals in the crystals. Backgrounds from more remote external sources such as the surrounding rock material and cement floor will also have effects on the crystals. Random coincidences of radiation from different background sources with two-neutrino double beta $(2\nu\beta\beta)$ decay of ^{100}Mo in $CaMoO_4$ will have the significant effect in the ROI. In this paper we report estimates of background counting rates due to the above mentioned background sources by performing simulations that investigate the effects of dominant background sources on the measured energy spectrum near the ROI.

2. The AMoRE-I Experiment

2.1. The geometry for detector simulation

The detector geometry used for the AMoRE-I simulation includes the CMO crystals, the shielding layers internal to the cryostat, the external lead shielding box, and the outer rock walls of the Y2L cavity. An array of thirty-five CMO crystals is located inside the cryostat. Each crystal has a cylindrical shape with a 4.5 cm diameter, 4.5 cm height, and a mass of 310 g. The total simulated crystal mass in the simulation is 10.9 kg, originated from initial design of AMoRE-I experiment. The 35 crystals are arranged in seven vertical columns, each with five crystals stacked coaxially, with one center column surrounded by six external ones. The side, bottom and a portion of top surfaces of each crystal are covered by a 65 μm-thick Vikuiti Enhanced Specular Reflector film (former VM2000). As discussed above, each crystal is mounted in copper frames, which is very complicated and sophisticated in reality. In the simulation, simplified design of the copper supporting frame is used, as shown in Fig. 1. Ge wafer and its copper frame are located above each crystal and below the lowest crystals.

This whole crystal assembly is enclosed in a cylindrical 2-mm-thick lead superconducting magnetic shielding tube with top and bottom discs, which is made of ultra-low activity, ancient lead. A 10-cm-thick lead plate (diameter of 40.8 cm and mass of 148.3 kg) placed on 1-cm-thick copper plate, is located just above the CMO crystal assembly, to attenuate backgrounds from materials above crystals inside the cryostat, such as wires, temperature sensors, heaters, G10 glassfiber, and stainless steel tubes. The crystal assembly is contained inside of four concentric copper cylinders with a total Cu thickness of 10 mm, all within an outer stainless-steel vacuum cylinder that is 5 mm thick, as shown in Fig. 2. Sequential top plates of shields are connected with G10 tubes, which were made of woven fiberglass material with 12 cm-height, 2.5 cm-diameter ($\sim$25 g). The G10 tubes are known as a material with high radioactive background. In AMoRE-I simulation configuration, simple top plates without any features or structures except G10 tubes are used. Realistic structures and features will
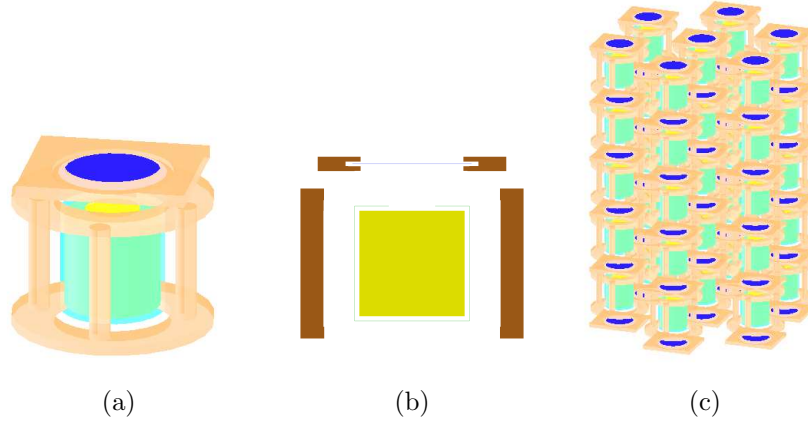
3

Figure 1: (a) CMO crystal (yellow) with Vikuiti reflector (light green) and CMO supporting copper frame (brown). On the top of reflector was open for a Ge wafer. (b) Vikuiti reflector surrounds each crystal except to center area. (c) 35 CMO crystals were stacked up 5 layers and 7 columns.

be positioned on each of the top plates for use in future simulations.

₆₀ The cryostat is located inside a 15-cm-thick external lead shield. The top plate of the lead shield is placed 50-cm above the lead shield and covers an area of 150×150 cm^2. To simulate the effects of radiation from the rock walls surrounding the experimental enclosure, the simulation uses a 50-cm-thick spherical rock shell. In alternative external shielding configuration, the effects of radia-₆₅ tion from the laboratory environment such as the cement floor, the laboratory walls and ceiling, and Iron supporting system, called a gantry, were simulated as shown in Fig. 3.

2.2. Simulation method

We have performed simulations using the GEANT4 Toolkit [4]. On internal ₇₀ or external materials, expected radioactive sources such as full decay chain of ^{238}U, ^{232}Th, and ^{235}U were simulated. Generally, most decay sources and products were considered to be in equilibrium state, thus all related activities within the chains are simply equal to ^{238}U, ^{232}Th, and ^{235}U activities multiplied by
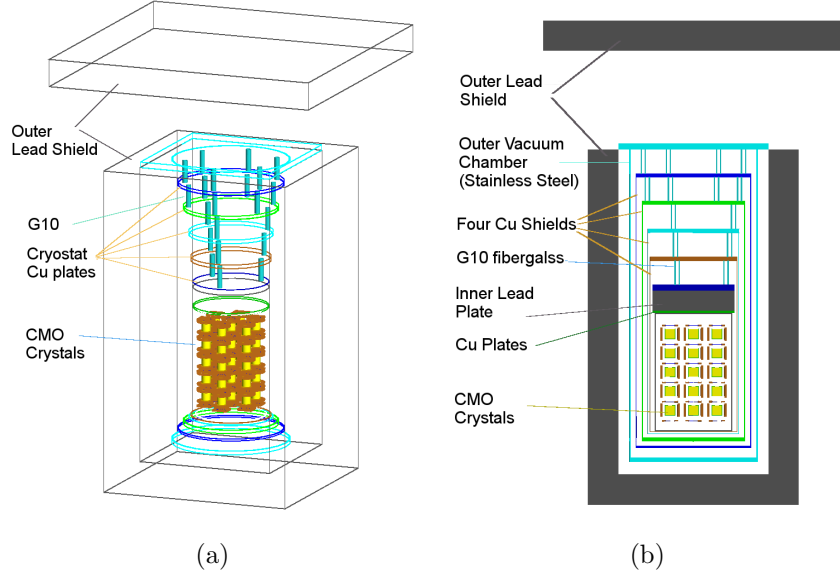
Figure 2: Outside the cryostat, a 15 cm-thick outer lead shield is located. The cryostat is composed of a stainless steel shield and four Cu shields. Top plates of cryostat shields are connected to G10 fiberglass (a) All the way inside the cryostat, the inner lead plate (grey) on the top of Cu plate is located above crystals. The 2-mm-thick superconducting lead shield surrounds crystals inside the cryostat.

the branching ratios for decay of the daughter isotopes. However, for ^{238}U de-
cays inside crystals, broken decay chain was considered by measured ^{238}U and ^{222}Rn concentrations separately. For background from rock, instead of ^{40}K and full decay chain simulation of ^{238}U and ^{232}Th nuclei, the highest energy γ such as 1.46, 1.87, and 2.61 MeV, respectively, were simulated at a rock shell, since daughter nuclei, α, and β can not penetrate the lead shield and the cryostat, made of stainless steel and copper shields.

Simulated each event includes deposits inside crystals within an event window of 100 ms when a decay occurs, so that decays with relatively short half lifetime such as, ^{212}Po decay with a half lifetime of 300 ns, have the followed
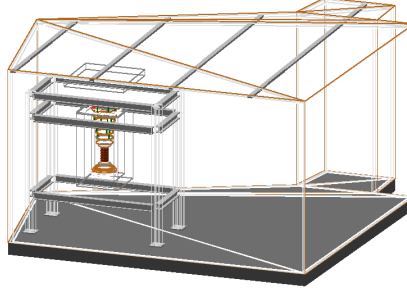
Figure 3: Cement floor, laboratory walls, ceiling of Y2L laboratory. Hollow steel poles (green) are on the wall and ceiling and between poles were filled with glass wool. Inner and outer of steel poles were covered by plaster board and steel plate in series.

decay within the same event, called pileup events. Pileup events within the event window are considered in simulated event. Furthermore, effect of random coincidence of ^{100}Mo $2\nu\beta\beta$ decay events and other radioactive sources inside crystals were estimated by convolution technique. For random coincidence rate calculation, ^{100}Mo $2\nu\beta\beta$ decay events were generated using an event generator, DECAY0 program [5] and those events were used as an input in our simulation package with AMoRE-I detector configuration to get a distribution of ^{100}Mo $2\nu\beta\beta$ decay inside CaMoO$_4$ crystals.

3. Analysis

For rare decay event searches one of the major concerns is background from external and internal sources. (i) First, since the internal background in CaMoO$_4$ crystals is a candidate of dominant background sources, internal background simulation from ^{238}U, ^{232}Th, ^{40}K, ^{235}U, and ^{210}Pb with full decay chains was carried out and their effect in the signal region was investigated. (ii) Second, backgrounds from materials in detector system including CMO support copper frame, Vikuiti reflector, superconducting lead shield, Cu plate under internal

6

lead, internal lead plate, G10 fiberglass, and outer lead shielding box, were simulated in AMoRE-I experimental configuration. (iii) Third, backgrounds from rock material and surrounding underground laboratory were simulated.

For backgrounds originated from decays outside of the cryostat such as, form the lead shielding box or rock shell, only γ de-excitations were found to produce signals in the crystal. Random coincidences of those radiations from different background sources are expected to be the main effect due to external sources in ROI. They are reported here explicitly for various external and internal sources.

Activities of ^{238}U, ^{232}Th, ^{40}K, and ^{235}U which were used to normalize the simulation results, were measured by germanium counting and inductively coupled plasma mass-spectroscopy (ICP-MS) technique. The High Purity Ge (HPGe) measurement were performed at Y2L. The ICP-MS measurements were all performed by the KAIST Analysis Center for Research Advancement (KARA), South Korea. The activity of backgrounds in a CMO crystal was measured by low temperature detector technique [6, 7]. The concentration of materials are listed in the following section.

3.1. Internal background in CaMoO$_4$

3.1.1. Background rate due to sources inside CaMoO$_4$

We simulated the full ^{238}U, ^{232}Th, and ^{235}U decay chains, as well as ^{40}K and ^{210}Pb, with contamination taken to be uniformly distributed inside the thirty-five crystals. The concentrations, listed in Table 1, were from a recent measurements of a CMO crystal [7], except a concentration of ^{232}Th. For concentration of ^{232}Th, more conservative upper limit is used than reported measurement. For 10^7 source events of each ^{238}U, ^{232}Th, and ^{235}U, and about 10^8 ^{210}Pb source events, background rate estimates were determined from the numbers of events in the ^{100}Mo $0\nu\beta\beta$ ROI, as shown in Table 1. Fig. 4 shows accumulated and each β-decay-induced events distribution. α event signal can be distinguished from signal of β and γ events by pulse shape discrimination (PSD) [6]. In this estimation, it was assumed that α event rejection power is 100%, so that β/γ-like events were considered as background sources.

7

Table 1: Concentrations based on a CMO crystal measurement [7] [mBq/kg]

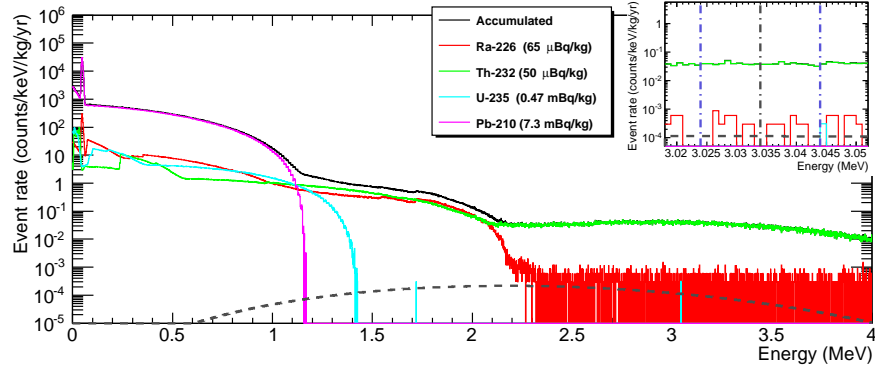|	^{210}Pb	^{238}U	^{226}Ra(^{222}Rn)	^{232}Th	^{235}U(^{211}Bi)
concentration	7.3	0.98	0.065	<0.05	0.47

Figure 4: Background β event rate due to ^{226}Ra, ^{232}Th, ^{235}U, and ^{210}Pb inside CMO crystals. The black line represents accumulated sum of all five distributions. Dashed line is due to random coincidence rate of two ^{100}Mo $2\nu\beta\beta$ decays.

Since α decaying at the surface of the crystal which deposit continuous energy lower than the initial alpha energy, the α-decay-induced event rate in ROI was appeared in Table 2. The β-decay-induced events are mostly from the ^{232}Th chain and originate from ^{208}Tl, ∼97.5%, and the rest β-decay-induced event from ^{232}Th chain are β-α pileup events from decays of (^{212}Bi+^{212}Po), which have half lifetime of 300 ns. All β decay-induced events of ^{238}U chain are β-α pileup events from decays of (^{214}Bi+^{214}Po), with a half lifetime of 164 μs.

3.1.2. Random coincidence rate of two ^{100}Mo $2\nu\beta\beta$ decays

The $2\nu\beta\beta$ decay in a CaMoO$_4$ approaches zero rate at the end-point energy, but random coincidence of these events can sum together (pileup) creating backgrounds for the $0\nu\beta\beta$ signal. The expected rate of $2\nu\beta\beta$ decay in a single CaMoO$_4$ crystal is 0.00284 counts/s, which is 1 double beta decay event per

8

Table 2: Background rate due to internal backgrounds (ckky)

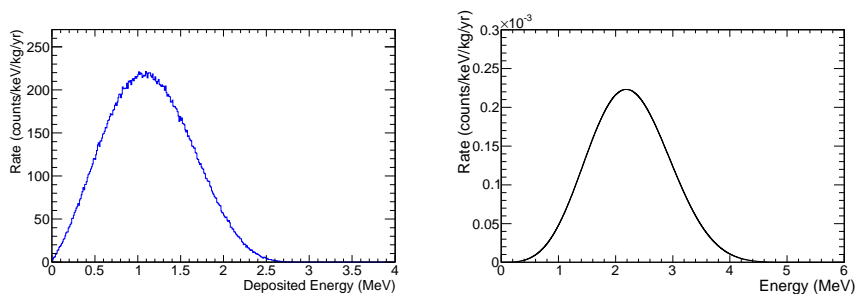|	^{210}Pb	^{238}U	^{226}Ra	^{232}Th	^{235}U
Total	0.017	0.0055	0.0013	0.0278	0.0055
α event rate	0.017	0.0055	0.00116	0.0005	0.0055
β event rate	0	0	0.00015	0.0273	0

~ 6 mins.

Figure 5: The energy distribution of ^{100}Mo $2\nu\beta\beta$ decay (left) and random coincidences of two $2\nu\beta\beta$ decays of ^{100}Mo (right). The random coincidence spectrum is derived by convolution of the $2\nu\beta\beta$ spectrum, and was normalized according to the $2\nu\beta\beta$ rate assuming an 0.5 ms coincidence window.

When 5×10^8 $2\nu\beta\beta$ events were simulated in the CaMoO$_4$ crystals (310 g each), corresponding to about 335 years of exposure, $\sim$99% of events have energy deposits in one crystal (single-hit events) and the remaining events ($<$1%) produced hits in multiple crystals. The random coincidence rate of two $2\nu\beta\beta$ decays was calculated by convolving two single-hit $2\nu\beta\beta$ decay energy distributions (see Fig. 5), and the accidental rate in 0.5 ms coincidence window, is 1.18×10^{-4} ckky in the ROI.

Random coincidence rates of ^{100}Mo $2\nu\beta\beta$ decay and each radioactive background source inside CaMoO$_4$ crystals such as ^{210}Pb, ^{238}U, ^{232}Th, ^{40}K, ^{235}U were calculated by convolving distributions. The concentration was from mea-

surements, shown in Table 1, and concentration of ^{40}K was assumed as 1 mBq/kg [8, 9]. The sum of random coincidence rates is Mo $2\nu\beta\beta$ decays and other nuclei was 7.80 $\times 10^{-6}$ ckky. In the same way, the random coincidence rates of two radioactive background sources inside CaMoO$_4$ crystals were calculated and the sum of rates between two background sources were 2.23 $\times 10^{-8}$ ckky.

3.2. Backgrounds from materials in detector system

3.2.1. Backgrounds from materials inside cryostat

Backgrounds from materials inside the cryostat around CaMoO$_4$ crystals, are another dominant background source candidates. As described earlier, Vikuiti reflector and CMO supporting copper frames are located near the crystals. Superconducting (SC) lead shield surrounds the detector system and inner lead plate and copper plates are above superconducting shield. G10 fiberglass are located between Cu shield plates of the cryostat. Concentration of Vikuiti reflector, measured by HPGe at Y2L [10], was 0.91 mBq/kg and 0.48 mBq/kg for ^{238}U (^{226}Ra) and ^{232}Th (^{228}Th), respectively. The CMO supporting copper frame was made of NOSV grade copper from Aurubis Co. and reported concentration of NOSV copper [11] is shown in Table 3. In order to reduce backgrounds from lead shields inside the cryostat, inner lead plate and superconducting lead shield, we purchased T2FA lead bricks from Lemer Pax with a certified activity of ^{210}Pb, 0.3 Bq/kg. Concentration of G10 glassfiber was measured by ICP-MS, as shown in Table 4.

Table 3: Concentrations of Vikuiti reflector [10] and NOSV copper [11]

	^{238}U (^{226}Ra)	^{232}Th (^{228}Th)	^{40}K
Vikuiti Reflector	<0.91 mBq/kg	<0.48 mBq/kg	<5.57 mBq/kg
CMO supporting copper frame	<16 μBq/kg	<25 μBq/kg	<88 μBq/kg
Cu plate under inner lead	<16 μBq/kg	<25 μBq/kg	<88 μBq/kg

10

Table 4: Concentrations in materials inside the cryostat

	^{210}Pb	^{238}U	^{232}Th	^{40}K
Inner lead plate	0.3 Bq/kg	1 ppt	1 ppt	-
G10 fiberglass	-	1732 ppb	12380 ppb	39 ppb
SC lead shield	0.3 Bq/kg	1 ppt	1 ppt	-
Outer lead shield	<59 Bq/kg	6.9 ppt	3.8 ppt	-

We simulated the effects of ^{238}U and ^{232}Th contaminants and their progeny, in the 65 μm-thick Vikuiti reflecting foils that surround the CaMoO$_4$ crystals. Simulated background rates in ROI due to β decay-induced events from these reflectors were 7.59×10^{-4} and 3.33×10^{-4} ckky for ^{238}U and ^{232}Th, respectively. All the β-decay-induced events in ^{238}U chain were β-α pileup events from decays of (^{214}Bi+^{214}Po) . In β-decay-induced events in ^{232}Th chain, 24% events were from decay of ^{208}Tl to ^{208}Pb and the rest events are β-α pileup events from decays of (^{212}Bi+^{212}Po). The rates were 7.6×10^{-5} and 1.04×10^{-4} ckky, for ^{238}U and ^{232}Th, respectively, applying 90 % β-α pileup event rejection.

When ^{238}U and ^{232}Th contaminants and their daughters are simulated in CMO support Cu frame, deposited energy distributions from β-decay-induced events were shown in Fig. 6. The β-decay-induced event rates in ROI from CMO support Cu frame are $<4.3 \times 10^{-7}$ and $<2.2 \times 10^{-4}$ ckky in ^{238}U and ^{232}Th chains, respectively. All the β-decay-induced events in ^{238}U chain were β-α pileup events from decays of (^{214}Bi+^{214}Po). In β-decay-induced events in ^{232}Th chain, 97% events come from decay of ^{208}Tl to ^{208}Pb and the rest events are β-α pileup events from decays of (^{212}Bi+^{212}Po).

For ^{238}U, ^{232}Th, and their progeny inside superconducting lead shield, the β-decay-induced-event rates in ROI was 2.9×10^{-6} and 7.9×10^{-6} ckky from ^{238}U and ^{232}Th decay chains, respectively. For ^{238}U and ^{232}Th inside inner lead plate and Cu plate under the lead plate, no events were found in ROI from simulated events, corresponding to a thousand of years or more, which
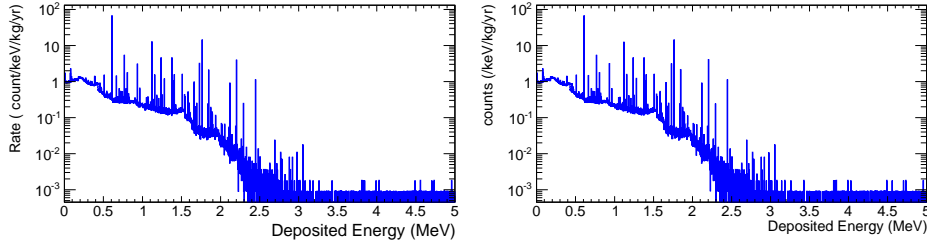
11

Figure 6: Deposited energy of single hit events from β decay chain in CMO crystals originated from (left) ^{238}U and (right) ^{232}Th in copper supporting frame.

resulted in the estimated upper limit (90% C.L.) in the order of 10^{-6} ckky. For ^{238}U and ^{232}Th sources in G10 fiberglass, the β-decay-induced-event rates in ROI was 3.15×10^{-6} and 4.3×10^{-6} ckky from ^{238}U and ^{232}Th decay chains, respectively.

Random coincidence rates of β/γ events from materials inside the cryostat with ^{100}Mo $2\nu\beta\beta$ decay were estimated, as well. The total random coincidence rate in ROI was in the order of $\sim 10^{-7}$-10^{-9} ckky for CMO supporting copper frame, SC lead shield, Cu plate, internal lead plate, which are less than random coincidence rate of two ^{100}Mo $2\nu\beta\beta$ decay inside the crystals.

3.2.2. Backgrounds from lead shielding box outside the cryostat

In order to attenuate γ-rays that originate from the surrounding rock a 15-cm-thick lead shielding box, ~ 15.6 ton, surrounds the cryostat. The JR Goslar lead bricks were purchased with a ^{210}Pb certification and was measured by ICP-MS for ^{238}U and ^{232}Th concentration and activities are listed in Table 4. In the outer lead shielding box, the expected rate of ^{210}Pb decay is 3.94×10^{13}/yr, when the concentration of ^{210}Pb in the lead shield is on level of 59 Bq/kg. When 5.63×10^9 ^{210}Pb events (~ 1.2 hr) were distributed inside lead shield and γ-rays with kinetic energy following a ^{210}Pb decay distribution, corresponding 1.68 $\times 10^{13}$ ^{210}Pb events (~ 0.43 yr), were generated on the inner surface of the lead shielding box, no events were found in the ROI. The total random coincidence rate of ^{100}Mo $2\nu\beta\beta$ decay for ^{210}Pb, ^{238}U, and ^{232}Th from outer lead shield was

3.64×10^{-6} ckky.

3.3. Backgrounds from rock material surrounding underground laboratory

The mono-energetic γ with kinetic energy of 2615 keV (emitted from ^{208}Tl in ^{232}Th chain), 1764 keV (from ^{214}Bi in ^{238}U chain), and 1461 keV (from ^{40}K) were generated in a rock shell. Reported concentrations of ^{238}U and ^{232}Th in rocks at Y2L were 2.1 and 13.0 ppm, respectively [12] and it was assumed that they were in the equilibrium state. The concentration of ^{40}K was 2.44 ppm, calculated with the natural abundance of K in rocks and natural abundance ratio of ^{40}K. When 1.38×10^9 events of ^{238}U and 2.21×10^8 events of ^{232}Th were simulated from the rock, corresponding to an exposure of 32.8 yr and 29.1 yr, respectively, no events were produced in the ROI and the estimated upper limit (90% C.L.) was 3.3×10^{-7} and 3.7×10^{-7} ckky. The total random coincidence rates of ^{100}Mo $2\nu\beta\beta$ decay with γ-rays from ^{238}U, ^{232}Th, and ^{40}K were 9.20 $\times 10^{-5}$ ckky.

3.4. Other backgrounds

- Concentration of samples of laboratory wall, called sandwich panel, and a cement floor was measured by ICP-MS, listed in Table 5. Although concentrations from the sandwich panel and cement floor were relatively high ($\sim$ppm), the effect from them is not significant due to lead shielding box and cryostat shield. For instance, for a ^{232}Th source, only 7.37×10^{-7}% events from sandwich panel and 9.63×10^{-7}% events from cement floor makes a hit on a crystal and no events were in ROI. The estimated random coincidence rate of ^{100}Mo $2\nu\beta\beta$ decays was in the or of 10^{-6} ckky.

Table 5: Concentrations in materials from laboratory environment

	^{238}U	^{232}Th	^{40}K
sandwich panel	1.51 ppm	1.25 ppm	202 ppt
cement floor	2.14 ppm	8.57 ppm	774 ppt

- Other sources of background (cosmogenic ^{88}Y, residual ^{48}Ca in the CMO crystals, and ^{214}Bi in the copper) are not expected to contribute significantly to the background near ^{100}Mo $0\nu\beta\beta$ decay signal region. Nevertheless, they will also be considered in the future.

4. Results

Estimated backgrounds of AMoRE-I for expected sources were summarized in Table 6. The most dominant background source was internal backgrounds in CaMoO$_4$ crystals.

Among the CaMoO$_4$ internal backgrounds, β-α events from ^{238}U and ^{232}Th chains can be rejected by PSD analysis, which was reported clear separation between α and β-decay-induced events with a prototype detector [6]. In this estimation, 90% rejection efficiency was used, conservatively. All β-decay-induced event rate in ^{238}U chain was β-α events from decays of (^{214}Bi + ^{214}Po), reduced to 1.5 $\times 10^{-5}$ ckky. In ^{232}Th chain, β-decay-induced events from ^{208}Tl decay (97.5% of β-decay-induced events in ^{232}Th chain) can be rejected using time correlations with the α signal from the preceding ^{212}Bi$\rightarrow^{208}$Tl α decay, called α-tagging method. Rejection of all events occur within 33 mins after a 6.207 MeV α event in the same crystal, results in a 97.4% veto efficiency for ^{208}Tl-induced β events in the ^{100}Mo $2\nu\beta\beta$ signal region, while introducing $\sim$1% dead-time. The rest 2.5% β-decay-induced events in ^{232}Thwere β-α events from decays of ^{212}Bi and ^{212}Po, rejected by PSD. In the end, β-decay-induced events in ^{232}Th in the CMO internal backgrounds reduced to 7.2 $\times 10^{-4}$ ckky.

For backgrounds from Vikuiti reflector and CMO supporting copper frames, the same event rejection methods were applied. β-α events of ^{238}U and ^{232}Th can be rejected by PSD. However, ^{208}Tl-induced β events rejection by 6.207 MeV α events did not work for events from Vikuiti reflector and copper frame, because no α particle from preceding ^{212}Bi$\rightarrow^{208}$Tl α decays arrived at the same crystal to β from ^{208}Tl decay. After β-α event rejection, the β-decay-induced events were reduced to1.8 $\times 10^{-4}$ for ^{238}U and ^{232}Th in Vikuiti reflector and

Table 6: Summary of α and β-decay-induced (β-like) backgrounds in major components estimated with measurements and simulation. Perfect alpha rejection and 90% β-α rejection are assumed.

Background sources	Isotopes	Simulated Time [Years]	Backgrounds in ROI [$\times 10^{-3}$ cnt/keV/kg/yr]		
			α events	β-like events	β-like events with cuts
Internal CMO	^{210}Pb	42.7	17.0	-	-
	^{238}U	35.3	5.51	-	-
	^{226}Ra	516	1.16	0.15	0.015
	^{232}Th	699	<0.54	<27.3	<0.72
	^{235}U	68.2	5.5	-	-
Vikuiti reflector	^{238}U	1684	9.41	<0.759	<0.076
	^{232}Th	3342	3.68	<0.333	<0.104
CMO supporting copper frame	^{238}U	4234	0.012	<0.0043	<0.0004
	^{232}Th	2842	0.0097	<0.22	<0.22
SC lead shield	^{238}U	9523	0.091	0.0029	0.0029
	^{232}Th	30354	0.0030	0.0079	0.0079
Inner lead shield	^{238}U	1466	-	<0.007	<0.007
	^{232}Th	1183	-	<0.009	<0.009
Cu Plate under inner lead	^{238}U	8746	-	<0.0013	<0.0013
	^{232}Th	25040	-	<0.0023	<0.0023
G10 fiberglass support tubes	^{238}U	24292	-	0.0026	0.0026
	^{232}Th	25040	-	0.0064	0.0064
Total			49.2	28.8	<1.18

2.25 $\times 10^{-4}$ ckky for ^{238}U and ^{232}Th in CMO supporting copper frame. In the end, the total expected rate in ROI due to direct background sources were <1.18 $\times 10^{-3}$ ckky.

Estimated backgrounds of random coincidence of two ^{100}Mo $2\nu\beta\beta$ decays with possible background sources were summarized in Table 7, including CaMoO$_4$ crys-
tals, Vikuiti reflector, CMO supporting copper frames, G10 fiberglass, outer lead shield, rock shell, etc. The dominant background source was two ^{100}Mo $2\nu\beta\beta$ decays inside the CaMoO$_4$ crystals, 1.18×10^{-4} ckky. Next dominant background source for random coincidence rate with ^{100}Mo $2\nu\beta\beta$ decay was γ from rock shell, due to its huge mass. The total estimated random coincidence rate of ^{100}Mo $2\nu\beta\beta$ decay with backgrounds was $<2.26 \times 10^{-4}$ ckky.

Table 7: Backgrounds due to random coincidence with ^{100}Mo $2\nu\beta\beta$ decay

Material	Sources	Random coincidence rate [$\times 10^{-3}$ cnt/keV/kg/yr]
Internal CMO	two ^{100}Mo $2\nu\beta\beta$ decays	0.118
	^{210}Pb,^{226}Ra,^{232}Th,^{40}K,^{235}U	<0.00780
	two radioactive sources	$<2.23 \times 10^{-5}$
Vikuiti reflector	^{238}U, ^{232}Th	$<1.14\times10^{-5}$
CMO supporting copper frame	^{238}U, ^{232}Th	$<3.08 \times 10^{-5}$
SC lead shield	^{210}Pb, ^{238}U, ^{232}Th	5.76×10^{-4}
Cu Plate	^{238}U, ^{232}Th	$<5.83\times10^{-6}$
Inner lead shield	^{210}Pb, ^{238}U, ^{232}Th	5.04×10^{-6}
G10 fiberglass	^{238}U, ^{232}Th, ^{40}K	4.08×10^{-4}
Outer lead shield	^{210}Pb, ^{238}U, ^{232}Th	0.00364
Cement floor	2.61 MeV γ (^{232}Th)	0.0017
Sandwich panel	2.61 MeV γ (^{232}Th)	0.0016
γ from Rock	1.76(^{238}U), 2.61 (^{232}Th) 1.46 MeV (^{40}K)	0.092
Total		<0.226

5. Discussion

The most dominant background source in ROI is β from ^{208}Tl decay in ^{232}Th chain inside CaMoO$_4$ crystals. In this estimation, we considered a conservative case of ^{232}Th concentration inside crystals, 50 μBq/kg, which was originated from the upper limit requirement for crystal growing. Concentrations of ^{238}U and ^{232}Th inside crystals are different in each crystal. Measured concentration of a CMO crystal did not have enough statistics of ^{232}Th events and only a limit of ^{232}Th was reported as <0.002 mBq/kg. If concentration of ^{232}Th inside crystals is lower than 50 μBq/kg, then the total background rate will be reduced. In case, with even crystals with concentration of $\sim$50 μBq/kg ^{232}Th, the AMoRE-I background goal can be achieved with 1% deadtime due to ^{208}Tl rejection.

For future experiment after AMoRE-I, reducing the effect of ^{208}Tl decay inside crystal is the most important. Therefore, purification of CaMoO$_4$ power and its growing process have been studied. In addition, methods for improving α-tagging efficiency of rejecting ^{208}Tl have studied using simulation. Currently, Vukiti reflector has used due to its high reflectivity, but searching for an alternative reflector with lower activities will be planned.

6. Conclusion

We simulated possible internal and external background sources in AMoRE-I configuration and the estimated total background rate in ROI was <1.41 $\times 10^{-3}$ ckky. The estimated background level of AMoRE-I experiment will achieve the goal, 2 $\times 10^{-3}$ ckky. For AMoRE-I, main background source was β from ^{208}Tl events inside the crystal and around material. In order to reduce background rate further, R&D for purification of crystal and material selection have been in progress.

References

[1] R. N. Mohapatra, et al., Theory of neutrinos: A White paper, Rept. Prog. Phys. 70 (2007) 1757–1867. `arXiv:hep-ph/0510213`, `doi:10.1088/0034-4885/70/11/R02`.

[2] C. Giunti, C. W. Kim, Fundamentals of Neutrino Physics and Astrophysics, Oxford, UK: Univ. Pr. (2007) 710 p, 2007.

[3] H. Bhang, et al., AMoRE experiment: a search for neutrinoless double beta decay of Mo-100 isotope with Ca-40 MoO-100(4) cryogenic scintillation detector, J. Phys. Conf. Ser. 375 (2012) 042023. `doi:10.1088/1742-6596/375/1/042023`.

[4] S. Agostinelli, et al., GEANT4: A Simulation toolkit, Nucl. Instrum. Meth. A506 (2003) 250–303. `doi:10.1016/S0168-9002(03)01368-8`.

[5] O. A. Ponkratenko, V. I. Tretyak, Yu. G. Zdesenko, The Event generator DECAY4 for simulation of double beta processes and decay of radioactive nuclei, Phys. Atom. Nucl. 63 (2000) 1282–1287, [Yad. Fiz.63,1355(2000)]. `arXiv:nucl-ex/0104018, doi:10.1134/1.855784`.

[6] G. B. Kim, et al., A CaMoO4 Crystal Low Temperature Detector for the AMoRE Neutrinoless Double Beta Decay Search, Adv. High Energy Phys. 2015 (2015) 817530. `doi:10.1155/2015/817530`.

[7] G. B. Kim, et al., in preparation.

[8] P. Belli, et al., New observation of 2beta 2nu decay of Mo-100 to the 0+(1) level of Ru-100 in the ARMONIA experiment, Nucl. Phys. A846 (2010) 143–156. `doi:10.1016/j.nuclphysa.2010.06.010`.

18

[9] D. Blum, et al., Search for gamma-rays following beta beta decay of Mo-100 to excited states of Ru-100., Phys. Lett. B275 (1992) 506–511. doi:10.1016/0370-2693(92)91624-I.

[10] D. S. Leonard, et al., in preparation.

[11] M. Laubenstein, G. Geusser, Cosmogenic radionuclides in metals as indicator for sea level exposure history, Appl. Rad. Isot. 67 (2009) 750. doi:10.1016/j.apradiso.2009.01.029.

[12] M. Lee, et al., Radon Environment in the Korea Invisible Mass Search Experiment and Its Measurement, J. Kor. Phys. Soc. 58 (2011) 713. doi:10.3938/jkps.58.713.